

Supplementary Materials for

Kinase domain dimerization drives RIPK3-dependent necroptosis

Saravanan Raju, Daniel M. Whalen, Meron Mengistu, Carter Swanson, John G. Quinn, Susan S. Taylor,
Joshua D. Webster, Kim Newton, Andrey S. Shaw*

*Corresponding author. Email: shaw.andrey@gene.com

Published 21 August 2018, *Sci. Signal.* **11**, eaar2188 (2018)
DOI: 10.1126/scisignal.aar2188

This PDF file includes:

- Fig. S1. Biochemical analysis of the RIPK3 kinase domain.
- Fig. S2. Characterization of *Ripk3*^{-/-} MEFs after reconstitution with WT RIPK3 and dimerization-defective RIPK3 mutations.
- Fig. S3. Expression of RIPK3 V36F does not cause apoptosis or TZ-dependent necroptosis.
- Fig. S4. Characterization and kinetics of FKBP-FRB RIPK3 fusion system for induced heterodimerization.
- Fig. S5. RIPK3-induced apoptosis by RIPK3 D161N and the RIPK3 inhibitor GSK'872.
- Fig. S6. Model of the mechanism of RIPK3 D161N function.

Figure S1

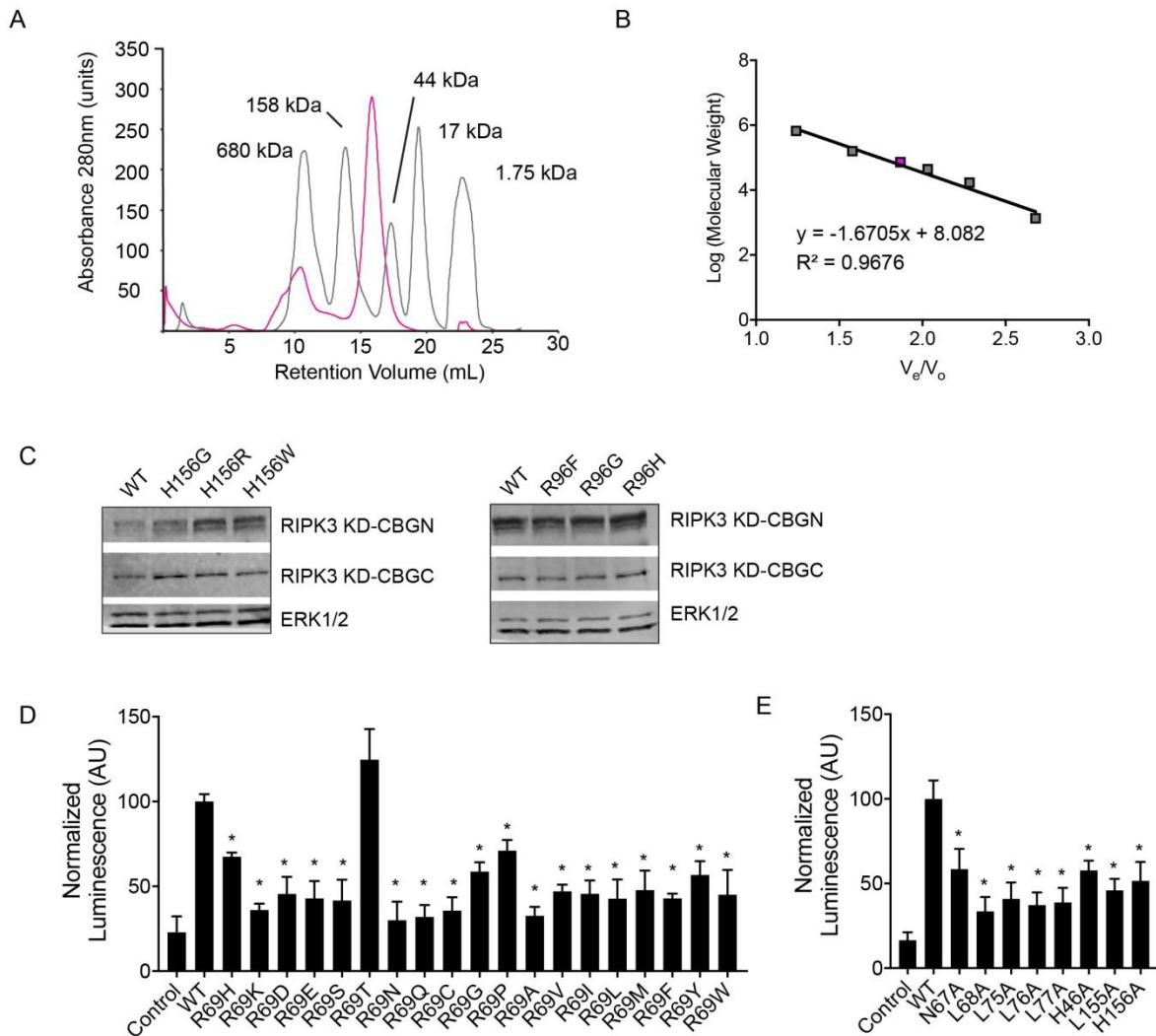


Fig. S1. Biochemical analysis of the RIPK3 kinase domain. (A and B) Size exclusion chromatography analysis of the molecular weight of purified MmRIPK3 kinase-domain (S2-H303) (red line) and molecular weight standards (grey). Images (A) are representative of 4 independent experiments. Logarithmic plot (B) of the Molecular Weight versus the ratio between elution volume (V_e) and column exclusion volume (V_o) for the standards (gray squares) and RIPK3 (purple square) are means from all experiments. (C) Western blot analysis of the indicated RIPK3 mutants in lysates of 293T cells co-transfected with RIPK3-CBGN and the indicated RIPK3-CBGC mutations. Blots are representative of 3 independent experiments. (D and E) Split luciferase complementation assay assessment of RIPK3 dimerization in 293T cells were transiently transfected with plasmids expressing WT RIPK3 kinase domain fused to the C-terminal domain of Click Beetle luciferase (RIPK3 KD-CBGC) and with the indicated RIPK3 kinase domain mutations fused to the N terminus of Click Beetle luciferase (CBGN-RIPK3 KD). Luminescence data are means \pm SD of 8 replicates per condition pooled from X independent experiments. * $P > 0.05$ by Mann-Whitney test with Bonferonni correction.

Figure S2

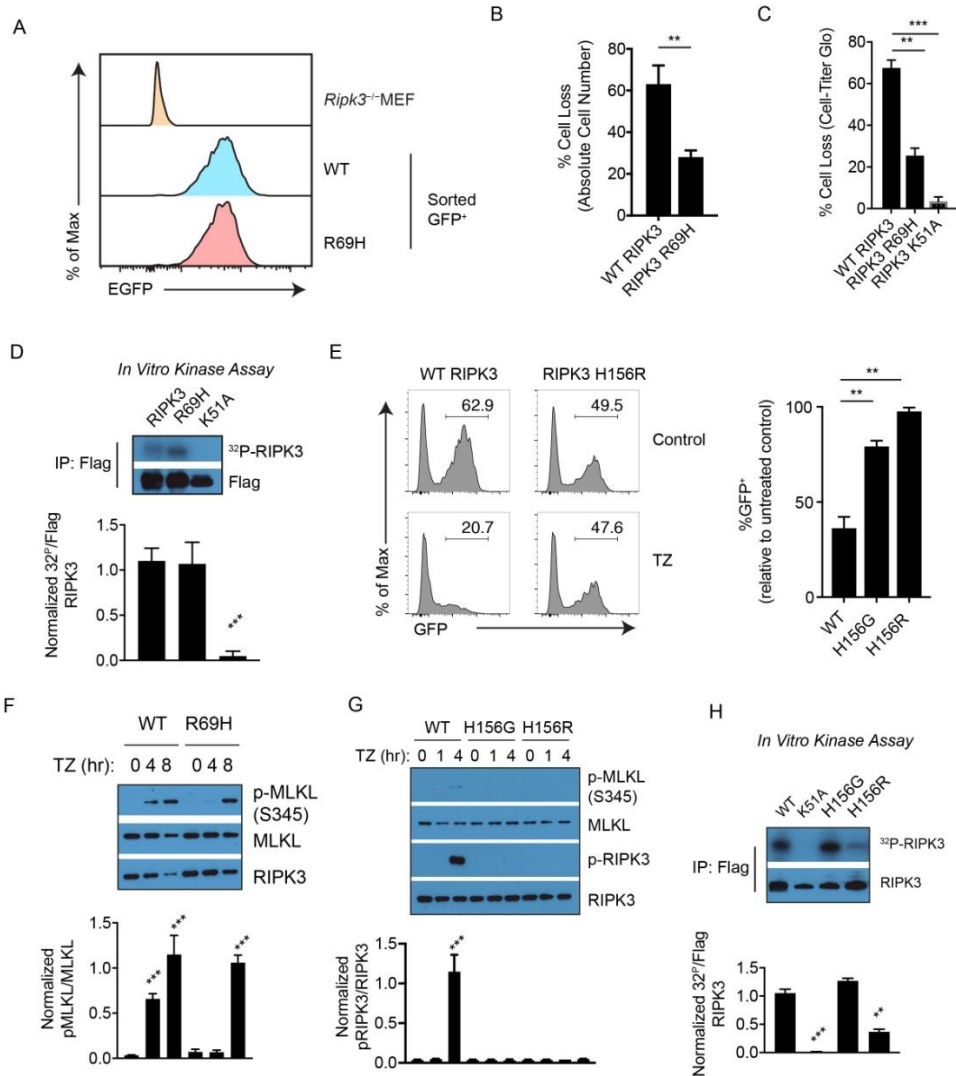


Fig. S2. Characterization of *Ripk3*^{-/-} MEFs after reconstitution with WT RIPK3 and dimerization-defective RIPK3 mutations. (A) Flow cytometry of *Ripk3*^{-/-} MEFs and transduced MEFs sorted for homogenous EGFP expression from Figure 3. (B, C) Cell Loss following TZ treatment of cells from A as measured by (B) number of live cells remaining following treatment and (C) as measured by Cell-Titer Glo. (D, H) 293T cells were transfected with the indicated pcDNA3-Flag-RIPK3 constructs and 48 hours later subject to immunoprecipitation with Flag antibody and an *in vitro* kinase assay using [γ -³²P]-ATP. Reactions were analyzed via ³²P autoradiography and immunoblotting. (E) *Ripk3*^{-/-} MEFs were infected with lentiviruses encoding EGFP-P2A-RIPK3 WT or indicated mutations. Cells were treated with TZ for 24 hours and were analyzed by flow cytometry for expression of EGFP (left panel). Quantification of EGFP⁺ cells relative to untreated control (right panel). (F, G) RIPK3 WT and (F) RIPK3 R69H or (G) H156G and R expressing cells were treated with TZ for the indicated times. Cell lysates were prepared directly used for immunoblotting. Data are shown as means and standard deviation (B, C, E) and are representative of at least 3 independent experiments. **P<0.01, ***P<0.005 by Student's t-test.

Figure S3

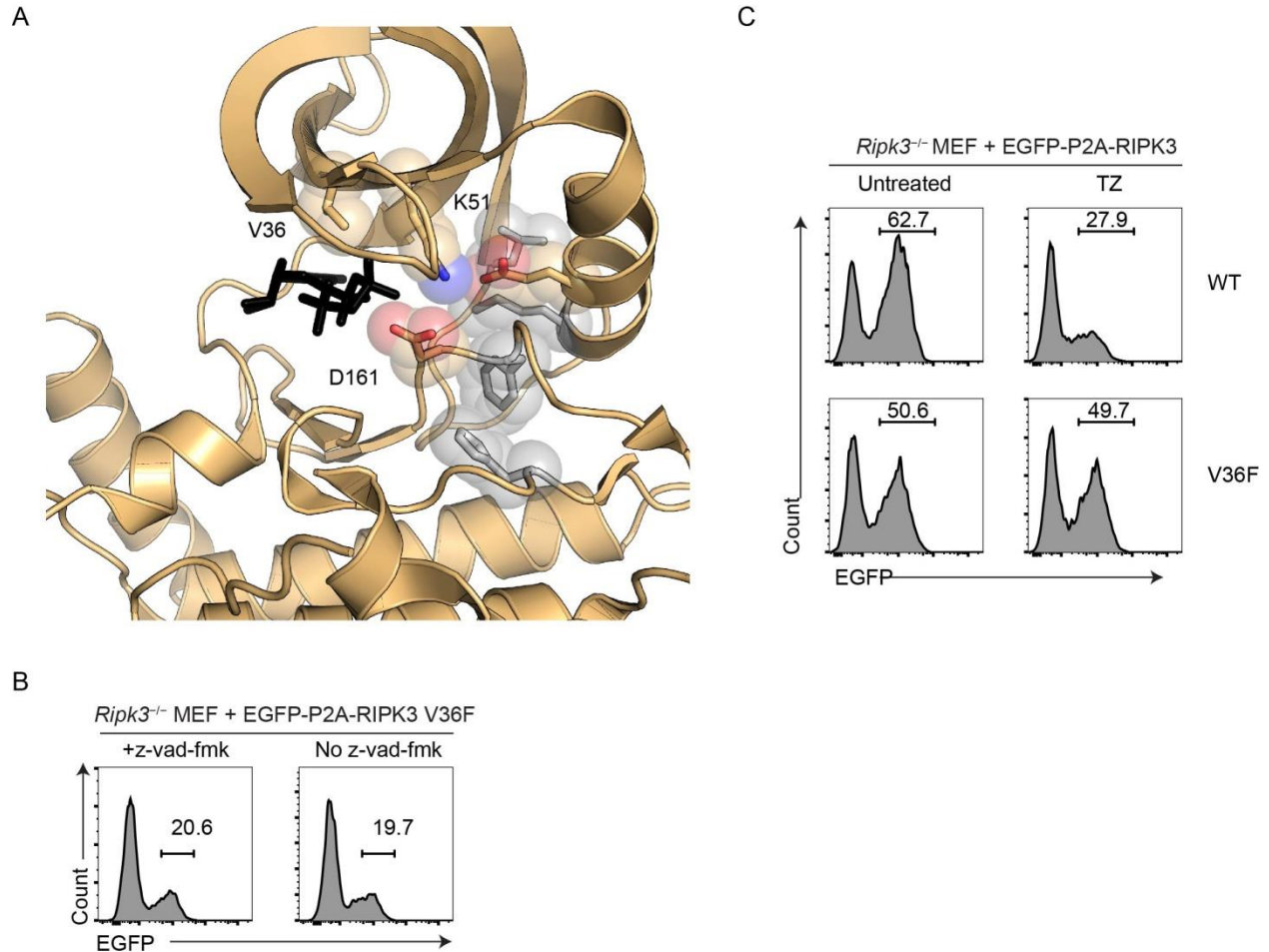


Fig. S3. Expression of RIPK3 V36F does not cause apoptosis or TZ-dependent necroptosis. (A) Structure of the RIPK3 kinase domain (amber; PDBID: 4M66) indicating residues V36, catalytic residues K51 and D161. R-spine residues are displayed in gray and ATP is included as black sticks. (B and C) Flow cytometry analysis of EGFP expression in *Ripk3*^{-/-} MEFs transduced with the indicated EGFP-P2A-RIPK3 construct and treated with TZ (B) or z-vad-fmk (C) as indicated 24 hours before analysis that were immunoprecipitated for Flag. Data (B to C) are representative of at least 3 independent experiments.

Figure S4

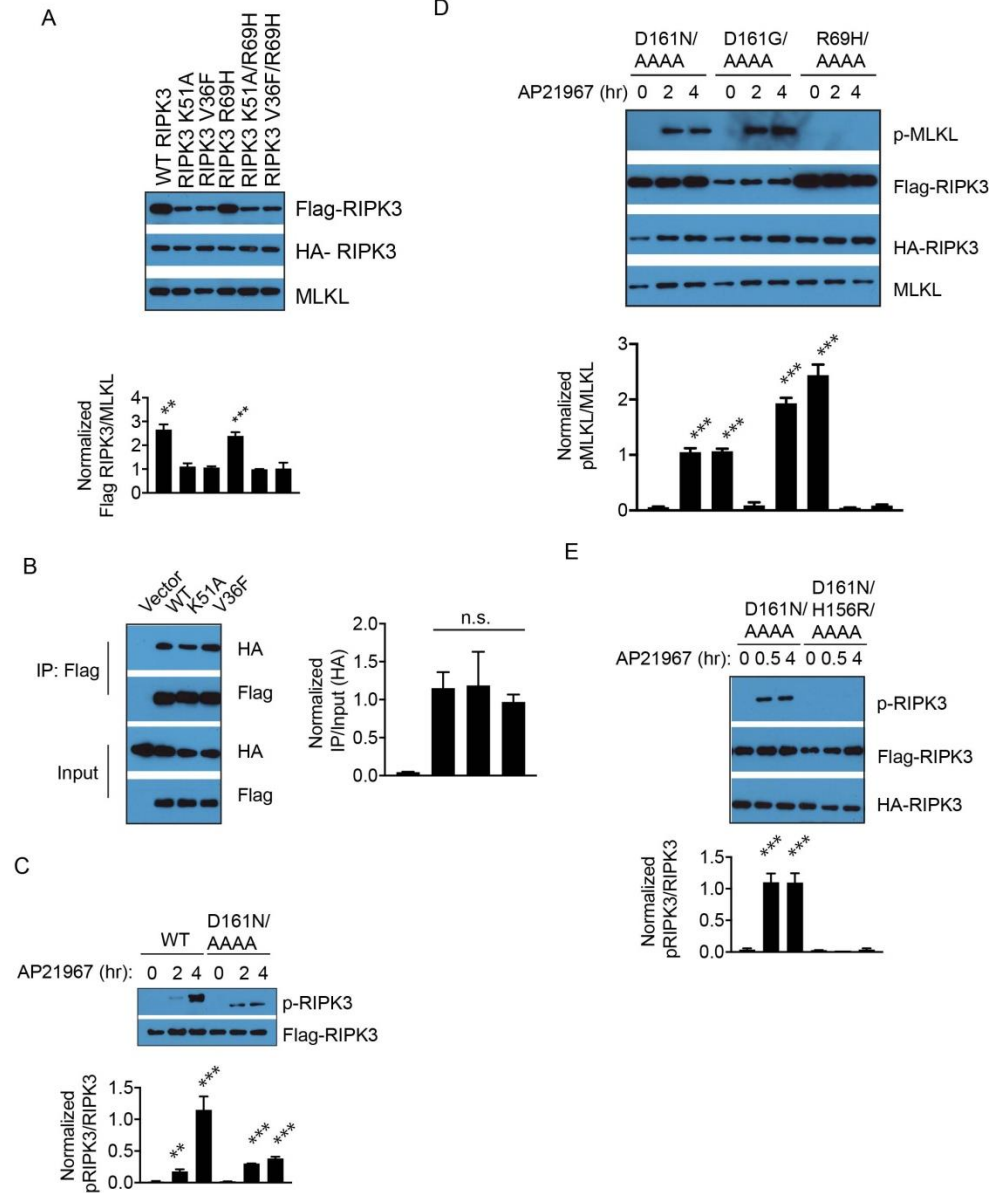


Fig. S4. Characterization and kinetics of FKBP-FRB RIPK3 fusion system for induced heterodimerization. (A) Western blot analysis for the indicated proteins in cell lysates from mCherry⁺EGFP⁺ sorted *Ripk3*^{-/-} MEFs co-transduced with lentiviral constructs EGFP-P2A-HA-WT RIPK3-FRB* and mCherry-P2A-2xFlag-RIPK3 WT-FKBP or mutants of RIPK3. (B) Co-immunoprecipitation analysis of RIPK3 Kinase domain (1-313aa) interactions in lysates of 293T cells co-transfected with pcDNA3-Flag-RIPK3 Kinase Domain and the indicated pcDNA3-HA-RIPK3 Kinase Domain (C to E) Western blot analysis for the indicated proteins in lysates from RIPK3 D161N/AAAA-FKBP or indicated mutants and RIPK3 WT-FRB* expressing cells were treated with z-vad-fmk for 1 hour followed by AP21967 for the indicated times. All blots are representative of at least 3 independent experiments. Quantified data are means \pm SD from all experiments. **P<0.01, ***P<0.005 by Student's t-test.

Figure S5

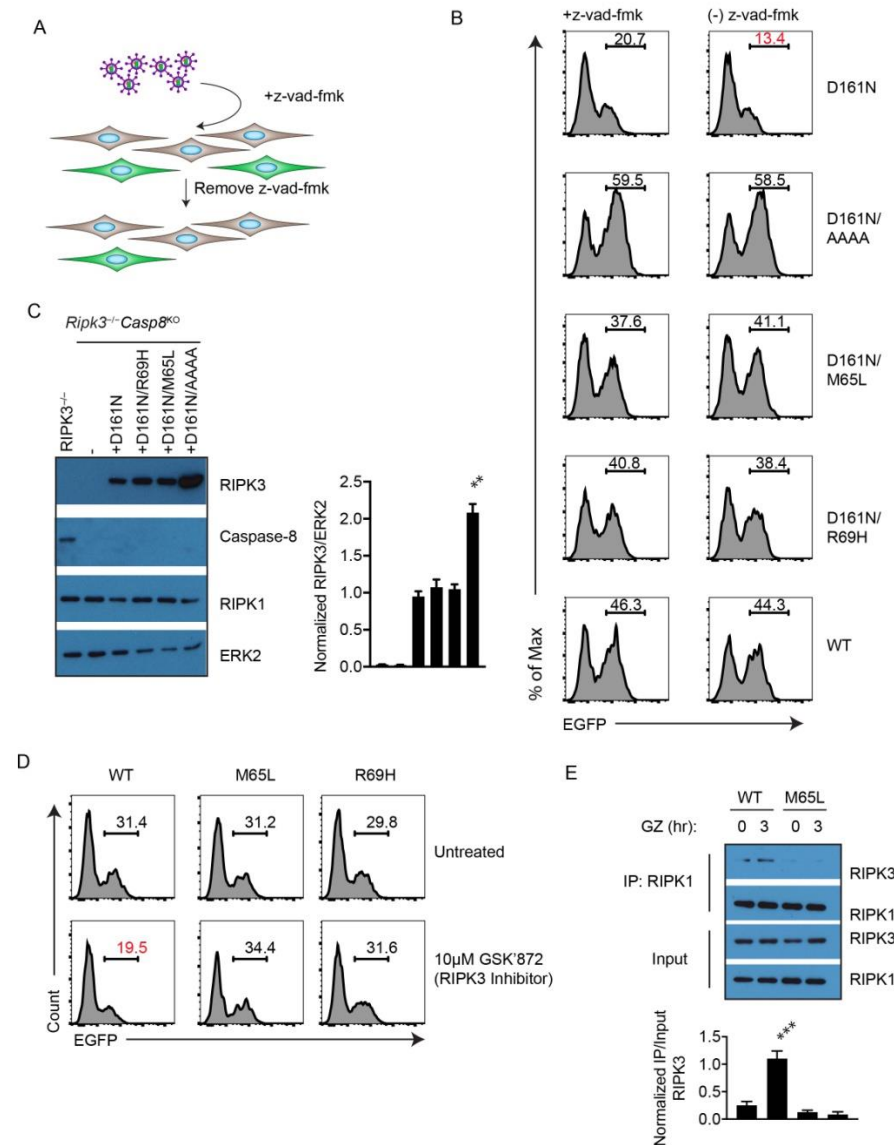


Fig. S5. RIPK3-induced apoptosis by RIPK3 D161N and the RIPK3 inhibitor GSK'872. (A) Schematic for simultaneous transduction of *Ripk3*^{-/-} MEFs with EGFP-P2A-RIPK3 and treatment with z-vad-fmk followed by quantification of cells undergoing apoptosis following removal of z-vad-fmk. (B) Flow cytometry analysis of EGFP expression in cells transduced with the indicated RIPK3 construct and treated with z-vad-fmk, as indicated. (C) Western blot analysis of RIPK3, Caspase-8, and RIPK1 in lysates of *Ripk3*^{-/-} and *Ripk3*^{-/-}*Caspase-8*^{KO} cells transduced with the indicated RIPK3 constructs and sorted for equivalent EGFP expression. (D) Flow cytometry of EGFP expression in cells *Ripk3*^{-/-} MEFs transduced with the indicated RIPK3 constructs and treated with GSK'872. (E) Co-immunoprecipitation analysis of RIPK3 interaction with RIPK1 in lysate of RIPK3 WT and RIPK3 M65L expressing cells were treated with the GSK'872 and z-vad-fmk for 3 hours that were immunoprecipitated for RIPK1. Data (B to E) are representative of at least 3 independent experiments. Quantified data (C, E) are means ± SD from all experiments. **P<0.01, ***P<0.005 by Student's t-test.

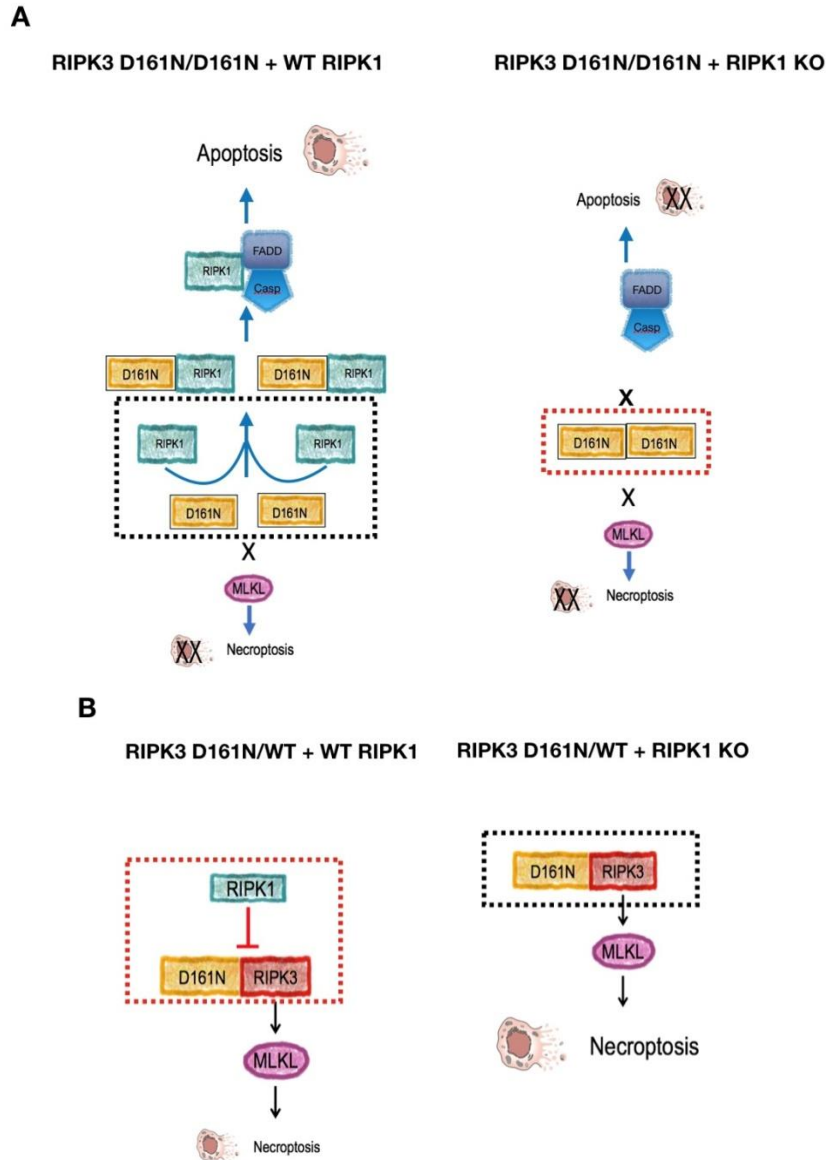


Fig. S6. Model of the mechanism of RIPK3 D161N function. **A.** Potential mechanism explaining D161N/D161N phenotypes. In the presence of RIPK1, RIPK3 D161N can form heterodimers resulting in activated RIPK1. Active RIPK1 induces apoptosis via a FADD/Caspase 8 dependent mechanism. In the absence of RIPK1, necroptosis doesn't occur because there is no active RIPK3 and apoptosis doesn't occur because RIPK1 isn't present. **B.** Potential mechanism explaining RIPK3 D161N/WT RIPK3 heterozygous phenotypes. In the presence of WT RIPK1, RIPK3 D161N/WT heterodimers do not form or are suppressed. In the absence of WT RIPK1, RIPK3 D161N is able to dimerize and activate WT RIPK3 to induce MLKL phosphorylation and necroptosis. Black dotted line box depicts active complexes. Red dotted line box depicts inactive complexes.